JOURNAL OF AIRCRAFT
Vol. 35, No. 2, March–April 1998

Hybrid Airfoil Design Method to Simulate Full-Scale Ice Accretion Throughout a Given α Range

Farooq Saeed,* Michael S. Selig,† and Michael B. Bragg‡
University of Illinois at Urbana–Champaign, Urbana, Illinois 61801-2935

A design procedure is presented for hybrid airfoils with full-scale leading edges and redesigned aft sections that exhibit full-scale airfoil water droplet-impingement characteristics throughout a given angle of attack or α range. The design procedure is an extension of a previously published method in that it not only allows for subcritical and viscous-flow analysis in the design but is also capable of off-design droplet-impingement simulation through the use of a flap system. The limitations of the flap-system-based design for simulating both on- and off-design full-scale droplet-impingement characteristics and surface-velocity distribution are discussed with the help of specific design examples. In particular, this paper presents the design of two hybrid airfoils at two different angles of attack, such that they simulate both the full-scale velocity distribution as well as droplet-impingement characteristics at the respective design angles of attack. Both of the hybrid airfoils are half-scale airfoil models with the nose section matching the full-scale coordinates of the Learjet 305 airfoil back to 5% chord on the upper surface and 20% chord on the lower surface. The effect of flap deflection and droplet size on droplet-impingement characteristics is also presented to highlight the important limitations of the present method both on- and off-design. This paper also discusses important compromises that must be made to achieve full-scale ice accretion simulation throughout a desired α range and suggests alternatives such as applying a multipoint design approach.

Nomenclature

c	= airfoil chord length
s	= airfoil surface arc length measured from the leading edge
T	= freestream static temperature
V	= surface velocity
$\bar{V}$	= surface velocity normalized by V_∞
V_∞	= freestream velocity
x, y	= airfoil coordinates
α	= angle of attack relative to the chord line
α_e	= effective angle of attack relative to the nose-section chord line, $\alpha - \gamma$
β	= local impingement efficiency
Γ	= circulation strength normalized by $V_\infty c$
γ	= nose droop angle
δ	= droplet diameter
δ_f	= flap deflection

Subscripts

fs	= full-scale airfoil
l	= lower surface
ss	= subscale airfoil
u	= upper surface

Introduction

RECENT aircraft accidents have raised important flight safety issues related to the operation of aircraft under severe weather conditions.[1-5] To improve flight safety a better understanding of the effect of ice accretion on the aerodynamic performance of modern airfoils is required. One important step in the process is to evaluate the aerodynamic performance of the airfoil sections, or the wing as a whole, at the icing conditions within the certification icing envelope that results in the largest performance penalties.

For aircraft safety one of the most important performance parameters is the maximum lift coefficient. Therefore, while drag and pitching moment are important, the icing condition that results in the largest degradation in maximum lift coefficient is the most critical. The determination of the critical ice accretion and its aerodynamic effect on a set of modern airfoils, typical of those in use on aircraft, is under way at NASA Lewis Research Center. The research reported here is part of this larger effort.

Because of the difficulties and uncertainties in ice accretion scaling,[6-11] testing at full-scale is desirable yet costly. Moreover, available ice accretion tunnels are too small to test full-scale airfoils or wings of most aircraft of interest. One way to expand the usefulness of existing icing tunnels and to facilitate testing of aircraft de-icing/anti-icing systems is to test hybrid airfoils or subscale airfoils with full-scale leading edges and redesigned aft sections, to provide full-scale icing conditions at the leading edge. The term *hybrid method* refers to using a full-scale leading edge to match the full-scale ice accretion. The aft section of the hybrid airfoil is specially designed to provide flowfield and droplet impingement similar to that on the full-scale airfoil leading edge. One such approach used airfoils with full-scale leading edges and truncated aft sections to simulate the flowfield of the full scale, thereby avoiding altogether the ice-accretion process on the airfoil leading edge and the associated scaling issues.[12] Interestingly, neither the approach nor its range of application received much attention, despite its numerous merits, such as permitting an in-depth study of droplet impingement and ice accretion on full-scale leading-edge sections within the capabilities of current icing research facilities. Moreover, the method may also prove useful for aircraft company icing certification.

Presented as Paper 97-0054 at the AIAA 35th Aerospace Sciences Meeting, Reno, NV, Jan. 6–9, 1997; received May 15, 1997; revision received Sept. 15, 1997; accepted for publication Sept. 17, 1997.

*Graduate Research Assistant, Department of Aeronautical and Astronautical Engineering, 306 Talbot Laboratory, 104 South Wright Street. Student Member AIAA.

†Assistant Professor, Department of Aeronautical and Astronautical Engineering. Senior Member AIAA.

‡Professor, Department of Aeronautical and Astronautical Engineering. Associate Fellow AIAA.

In the absence of a systematic study to provide insight into the design of the aft section, a recent study was carried out in which a design procedure for hybrid airfoils was successfully developed and demonstrated with specific design examples.[13] The study showed that hybrid airfoils could be designed to exhibit the full-scale velocity distribution on its nose section as well as full-scale droplet-impingement characteristics and, therefore, ice accretion. An inherent limitation of the design procedure outlined in the study[13] is that the method was restricted to a single-point design and, therefore, lacked the capability to handle off-design cases. Moreover, the method used the matched lift coefficient technique to correct for viscous effects.

To overcome these limitations, the present study was carried out with the objective of expanding the scope of the single-point design procedure of Ref. 13 to a method that enables the hybrid airfoils to exhibit full-scale velocity distributions as well as droplet-impingement characteristics and, therefore, full-scale ice accretions throughout a desired α range.

The task of simulating off-design full-scale droplet impingement, as will be shown later, is successfully accomplished by introducing a plain flap on the hybrid airfoil. The use of a plain flap, however, fails to simulate full-scale velocity distribution at the off-design conditions. Because differences in the velocity distribution on the nose section will affect both the thermodynamics of ice accretion and droplet impingement on the surface, it therefore becomes necessary to simulate the full-scale velocity distribution in addition to droplet impingement at the off-design conditions. Thus, to simulate the full-scale velocity distribution as well as droplet-impingement efficiency on the nose section of the hybrid airfoil throughout a desired α range, it is necessary to formulate a multipoint hybrid airfoil design method.

To set the stage for the multipoint design method, this paper presents the design of two half-scale hybrid airfoils that are designed at two different angles of attack, such that they simulate the full-scale nose-section velocity distributions as well as the droplet-impingement characteristics at their respective design angles of attack. The velocity distribution and droplet-impingement characteristics of the two hybrid airfoils are then analyzed at an off-design angle of attack and compared with that of the full-scale airfoil. The results are then used to highlight the limitations of the present method and, therefore, suggest a need for a multipoint design method. Important compromises that must be made to achieve a multipoint design for full-scale ice-accretion simulation throughout a desired α range are also discussed.

Design Approach

The hybrid-airfoil design procedure for the full-scale flowfield and droplet-impingement simulation uses both validated computational airfoil aerodynamics and droplet-impingement codes,[14-29] specifically, an inverse design method,[16] the Eppler code,[17-19] XFOIL,[22] and AIRDROP.[27] Reference 13 provides a brief discussion of each of these codes. For a more detailed discussion, the reader is referred to the associated literature.

Unlike the method presented in Ref. 13, wherein the potential flow is corrected for viscous effects using the matched lift coefficient technique, the present method uses a modified version of XFOIL. The modified version of XFOIL was obtained by integrating the droplet-trajectory and droplet-impingement calculation subroutines from the AIRDROP code into XFOIL. This was done to take advantage of XFOIL's ability to analyze both inviscid/viscous flow and incompressible/subcritical flows (unlike the AIRDROP code, which is based on an incompressible flow formulation). In this paper, the modified version of XFOIL is referred to as the XFOIL/AIRDROP code. Once the flowfield is determined using known flight and icing conditions, the droplet-trajectory calculation subroutines are then used in conjunction with the flow-solver subroutines to determine the droplet-impingement characteristics of the airfoil.

A conceptual illustration of the hybrid airfoil design procedure is shown in Fig. 1. A brief summary of these steps follows. First, a full-scale airfoil geometry is selected and the desired flight and icing conditions are specified. In particular, the Learjet 305 airfoil (Fig. 2) is used in this study to demonstrate the design procedure. The XFOIL/AIRDROP code is then used to predict the limits of droplet impingement on the full-scale airfoil. These full-scale limits of impingement are then used to establish how much of the full-scale upper and lower surfaces are used for the subsequent hybrid airfoil shapes. As in Ref. 13, this leading-edge section, which uses the full-scale coordinates, will be referred to as the nose section, and the remaining section of the hybrid airfoil profile will be referred to as the aft section. The aft section of the hybrid airfoil is then designed to provide full-scale flowfield and droplet-impingement characteristics on the nose section of the hybrid airfoil.

An initial geometry for the aft section is obtained through the use of PROFOIL, a multipoint inverse airfoil design code.[16] The design of the intermediate airfoil, from which the aft section of the hybrid airfoil is derived, is governed by several constraints, namely, the scale of the hybrid airfoil, the upper and lower surface thickness and slope at the junction between the nose and aft sections, and a desired form for the pressure recovery characteristics. Apart from these constraints, additional continuity and closure constraints that form an integral part of the inverse design methodology are also satisfied to achieve a physically realizable design.[16] A multidimensional Newton iteration scheme is employed to satisfy these constraints.

The flow over the hybrid airfoil is then analyzed using the XFOIL/AIRDROP code. To have a physically similar flow in the vicinity of the nose section of both the hybrid and the full-scale airfoils, the analysis is performed at the same angle of attack relative to the nose-section chord of both airfoils. The local velocity distributions over the nose section and the stagnation point locations on both the hybrid and full-scale airfoils are then compared. If the desired velocity distribution over the nose section and stagnation point location are not achieved, the aft section of the hybrid airfoil is redesigned and again merged with the nose section to form a new hybrid airfoil. The

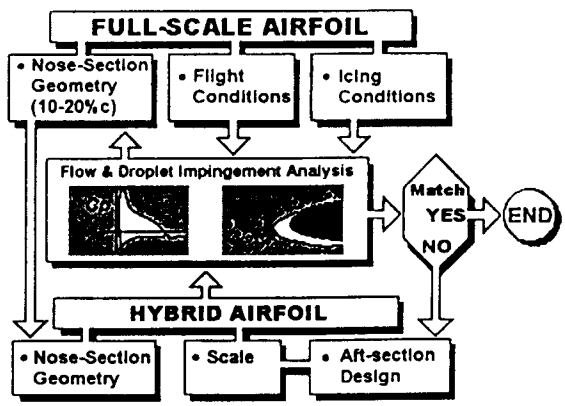

Fig. 1 Flowchart for the hybrid airfoil design procedure.

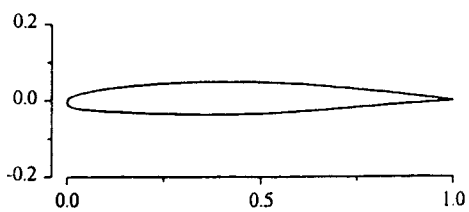

Fig. 2 Learjet GLC 305 airfoil.

flow over the new hybrid airfoil is then analyzed and compared with that of the full-scale airfoil. The process is repeated until the desired velocity distribution over the nose section is achieved.

In the next step, the droplet trajectories and impingement characteristics are determined from the XFOIL/AIRDROP code. The individual droplet trajectories are combined to calculate the droplet-impingement characteristics of the airfoil. The droplet-impingement characteristics of both the full-scale and hybrid airfoil are then compared. If the agreement in the droplet-impingement characteristics is poor, the hybrid airfoil is modified and the design process is repeated again until good agreement is reached. At this stage, the single-point design is accomplished. To achieve off-design full-scale ice accretions or droplet-impingement characteristics, a plain flap is employed on the hybrid airfoil. Thus, by deflecting the flap, the desired droplet-impingement characteristics are achieved over the hybrid airfoil for the off-design cases.

The off-design cases reveal, as will be shown in the next section, certain important limitations of the design method. These limitations include 1) the onset of flow separation on the hybrid airfoils at moderate to high angle of attack conditions, and 2) a mismatch in the velocity distribution on the nose section at off-design angles of attack. The former limitation can be improved either by using a more sophisticated flap system or by applying less conventional techniques, such as boundary-layer control through slot suction[30,31] or circulation control through trailing-edge blowing. The latter, however, is an important limitation of the present design method and can be overcome by using a multipoint design approach.

As mentioned earlier, the current study is an extension of the subscale airfoil design method first presented in Ref. 13. Reference 13 not only indicates that the subscale airfoil design method uses validated computational aerodynamic and droplet-impingement codes but also cites additional references in which these codes have been successfully applied to the design and analysis of airfoils for various applications and, thus, establishes the accuracy of numerical results it presents, as well as those presented in this paper.

Implementation

In this section, the effects of various parameters on two single-point airfoil designs are discussed. In particular, two half-scale hybrid airfoils were designed at different angles of attack such that they simulated both the full-scale velocity distribution on the nose section as well as droplet-impingement characteristics at the design conditions (single-point design). The off-design full-scale velocity distribution and droplet-impingement characteristics of each hybrid airfoil are compared to highlight important limitations of the present method.

Single-Point Design and Simulation

The design of two half-scale models of the GLC 305 airfoil that simulate full-scale velocity distribution and droplet-impingement characteristics is presented. Of the two hybrid airfoils, hybrid airfoil A is designed to simulate full-scale ice accretion at α = 2 deg, and hybrid airfoil B is designed to simulate full-scale ice accretion at α = 6 deg, along with the following icing conditions: V_∞ = 90 m/s (175 kn), $T = -10$°C, $Re = 6 \times 10^6$, M = 0.28, and VMD = 20 μm (where VMD = volume median droplet diameter). Although it is realized that in flight the conditions will change with the angle of attack, the conditions for both angles of attack are held constant here to simply illustrate the method.

As a first step, the droplet-impingement efficiency β for the GLC 305 airfoil that corresponds to the given flight and icing conditions is determined by the XFOIL/AIRDROP code. The results are shown in Fig. 3. For α = 6 deg, the XFOIL/AIRDROP code predicts the maximum limits of impingement as s_u = 0.0076 (x/c = 0.002) on the upper surface and s_l = −0.1822 (x/c = 0.174) on the lower surface. Because the limits of impingement define the surface over which ice will accrete on the airfoil, only that part of the full-scale airfoil geometry needs to be fixed as the nose section for the hybrid airfoil. Thus,

Table 1 Design flight and icing conditions

Variable	Full scale	Hybrid A	Hybrid B
V_∞, m/s	90	90	90
T, °C	−10	−10	−10
Re	6×10^6	3×10^6	3×10^6
M	0.28	0.28	0.28
c, m	1.0	0.5	0.5
VMD, μm	20	20	20
α, deg	2, 6	2	6
γ, deg	0	−1.5	−3
α_f, deg	2, 6	3.5	9

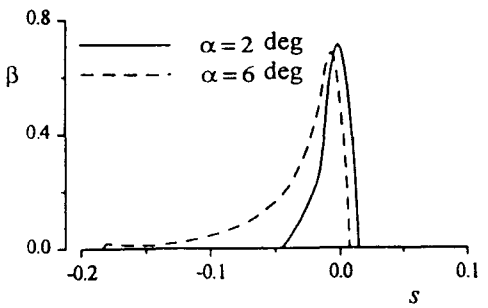

Fig. 3 Droplet impingement efficiency for the Learjet GLC 305 airfoil.

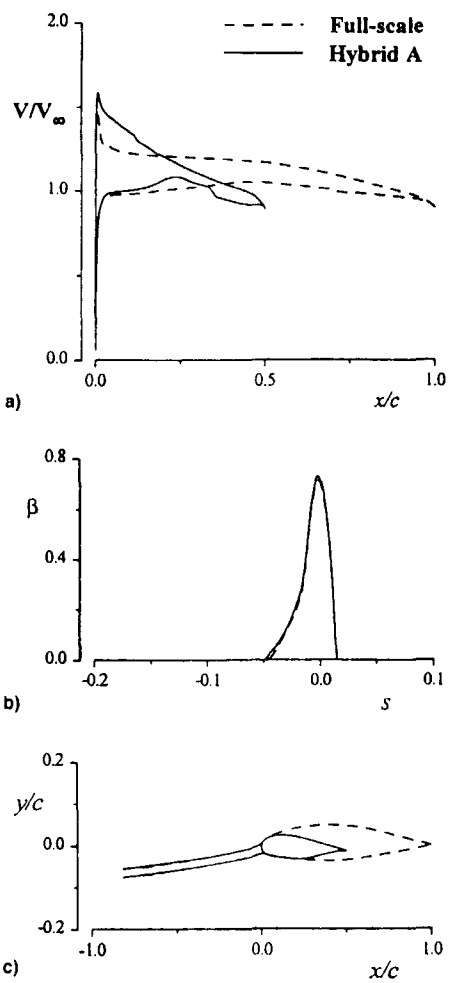

Fig. 4 Comparison of full-scale and hybrid airfoil A at design α = 2 deg: a) V_∞, b) β, and c) tangent droplet trajectories.

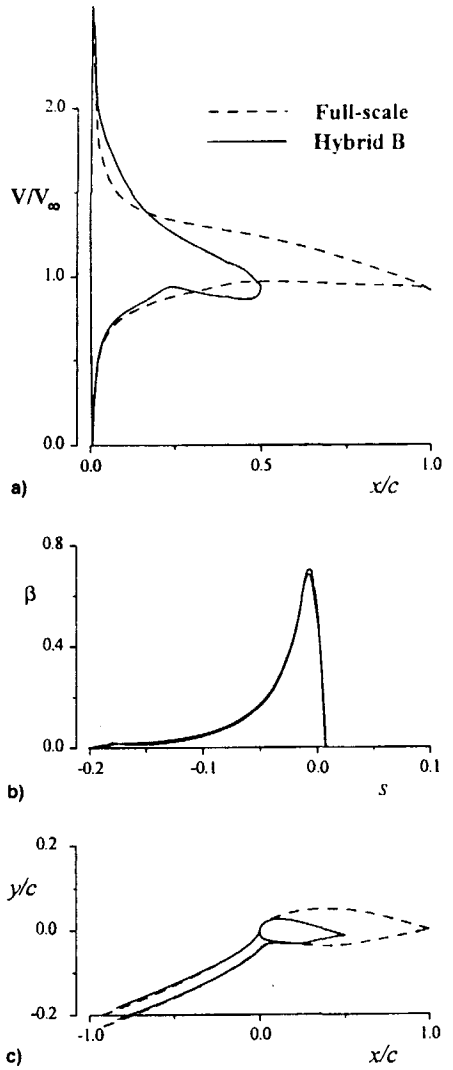

Fig. 5 Comparison of full-scale and hybrid airfoil B at design α = 6 deg: a) V_∞, b) β, and c) tangent droplet trajectories.

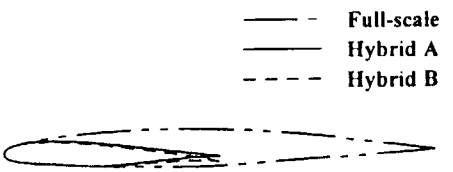

Fig. 6 Two hybrid airfoils and the Learjet GLC 305 airfoil.

the nose-section geometry for both hybrid airfoils was selected as the full-scale airfoil surface from x/c = 0.05 on the upper surface to x/c = 0.20 on the lower surface. The two hybrid airfoils were then designed following the procedure illustrated in Fig. 1. Table 1 lists the flight and icing conditions for the final single-point design.

A comparison of the full-scale airfoil velocity distribution with that of the individual hybrid airfoil velocity distributions (Figs. 4a and 5a) at the single-point design conditions shows good agreement over the common nose section. Comparisons of the impingement characteristics (Figs. 4b and 5b) and tangent droplet trajectories (Figs. 4c and 5c) also indicate excellent agreement with those of the full-scale airfoil. The tangent droplet trajectories, although originating from different locations upstream, are matched in the vicinity of the leading edge. This is consistent with the observations made during the case studies in Ref. 13. At this point, the single-point design for full-scale velocity distribution and droplet-impingement simulation is complete, and the two hybrid airfoils along with the Learjet 305 airfoil are shown in Fig. 6.

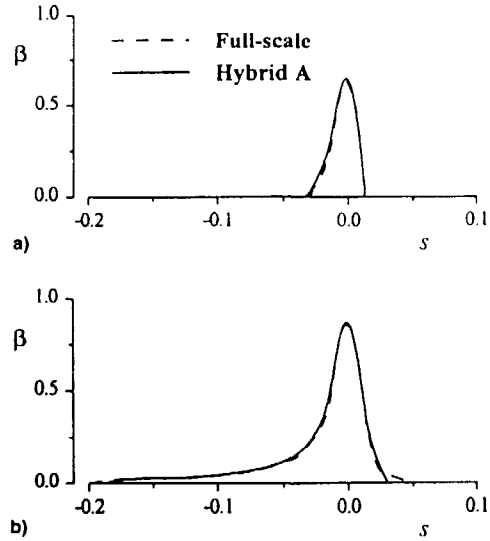

Fig. 7 Comparison of full-scale and hybrid airfoil A droplet-impingement efficiencies for design α at a) 5- and b) 40-μm droplets.

Effect of Droplet Size

The droplet-impingement characteristics of an airfoil, i.e., the limits of droplet impingement, β, and the maximum point on the β curve (referred to as β_{max}), depend to a large extent on the size of the water droplets in the flow. For the case of small droplets, the droplet drag dominates and the particles are very responsive to the flowfield and, therefore, act almost as flow tracers; whereas, in the case of large droplets, the droplet inertia dominates and the particles are less sensitive to changes in the flowfield. Changes in flow velocity for constant droplet size follow a similar trend. Thus, an increase in the droplet size or the flow velocity results in an increase in β, β_{max}, and the limits of droplet impingement. It is therefore interesting to examine the effect of different droplet sizes on full-scale droplet-impingement characteristics at constant flow velocity. Because, in natural icing clouds, the water droplets have volume median diameters ranging from 5–40 μm, the impingement characteristics of hybrid airfoil A were determined for two different droplet sizes. The results are presented in Fig. 7 and show good agreement where the droplet sizes are less than that selected for the single-point design. For larger droplet sizes, a good overall agreement can be seen, but the limits of β and β_{max} differ slightly. Similar results were also observed in hybrid airfoil B.

Off-Design Simulation

To simulate full-scale ice-accretion or droplet-impingement characteristics throughout a desired α range, a flap system was employed on each of the hybrid airfoils. The objective was to match both the velocity distribution and the droplet-impingement characteristics at any off-design angle of attack by an appropriate amount of flap deflection. To accomplish this task the two hybrid airfoils were analyzed at off-design angles of attack; in particular, hybrid airfoil A, designed to simulate conditions at α = 2 deg, was analyzed at α = 6 deg, and hybrid airfoil B, designed to simulate conditions at α = 6 deg, was analyzed at α = 2 deg. Other flight and icing conditions were kept the same as shown in Table 1. The results are shown in Figs. 8 and 9, in which the hybrid airfoil velocity distribution and droplet-impingement characteristics are shown with and without the appropriate flap deflection necessary to simulate full-scale droplet-impingement characteristics. The results show that, although the use of a flap on hybrid airfoils can be quite effective in simulating full-scale droplet-impingement characteristics at an off-design condition (the β curves for the

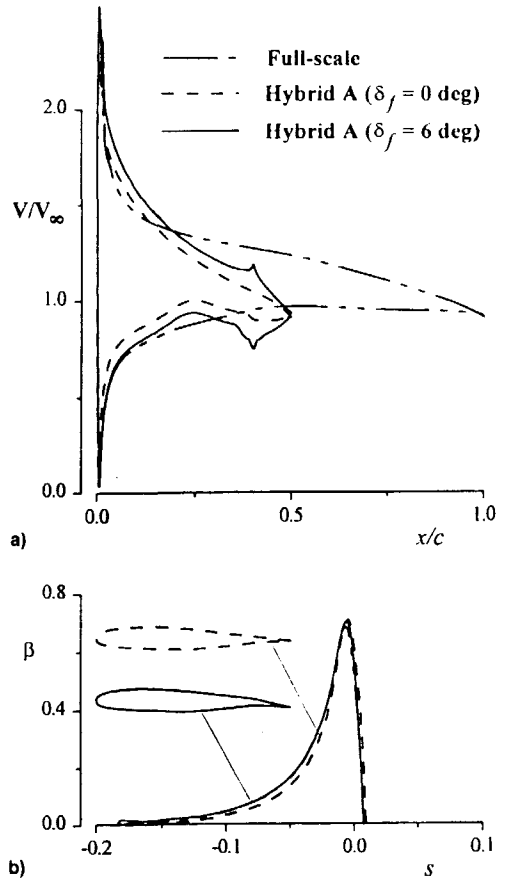

Fig. 8 Comparison of full-scale and hybrid airfoil A at off-design α = 6 deg: a) V_∞ and b) β, with and without flap deflection.

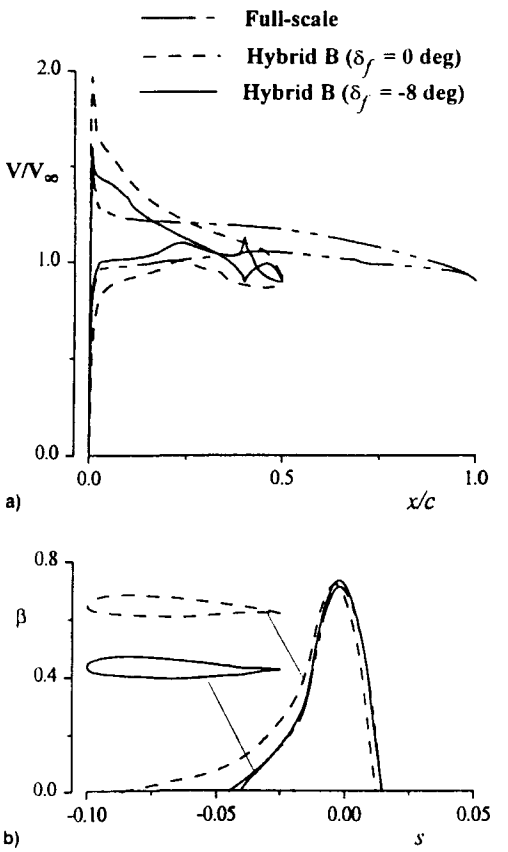

Fig. 9 Comparison of full-scale and hybrid airfoil B at off-design α = 2 deg: a) V_∞ and b) β, with and without flap deflection.

full-scale and hybrid airfoils are coincident), the flap does not yield the full-scale velocity distribution over the hybrid-airfoil nose section.

To determine the optimum flap setting, the root-mean-square (RMS) difference in local impingement efficiency RMS_β and in normalized surface velocity $RMS_{\bar{V}}$ were calculated for different α and flap settings. Mathematically, RMS_β and $RMS_{\bar{V}}$ are defined by

$$RMS_\beta = \|\beta_h(s) - \beta_s(s)\| \tag{1}$$

$$RMS_{\bar{V}} = \|\bar{V}_h(s) - \bar{V}_s(s)\| \tag{2}$$

where $s_l \leq s \leq s_u$.

Figures 10a and 10b show the variation in RMS_β and $RMS_{\bar{V}}$, respectively, for different angles of attack and δ_f for the hybrid airfoil A designed for α = 2 deg, and Figs. 11a and 11b show similar plots for the hybrid airfoil B designed for α = 6 deg. The optimum flap deflection was then selected as the one that corresponds to the minimum value of RMS_β.

The optimum flap settings corresponding to each angle-of-attack case are plotted in Fig. 12a for clarity. Figure 12b, on the other hand, shows a comparison of the Γ of both hybrid

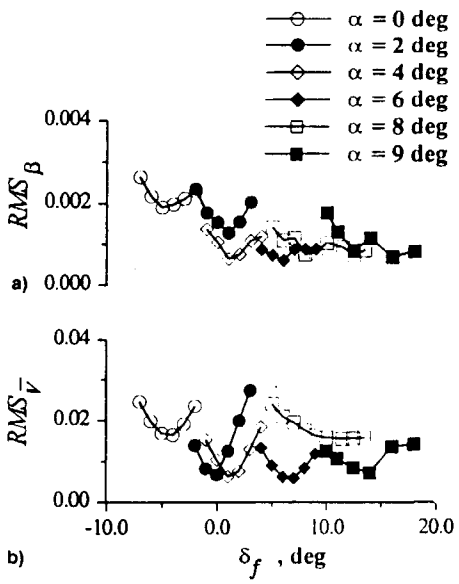

Fig. 10 Variation in the RMS values for different angles of attack and flap settings for hybrid airfoil A.

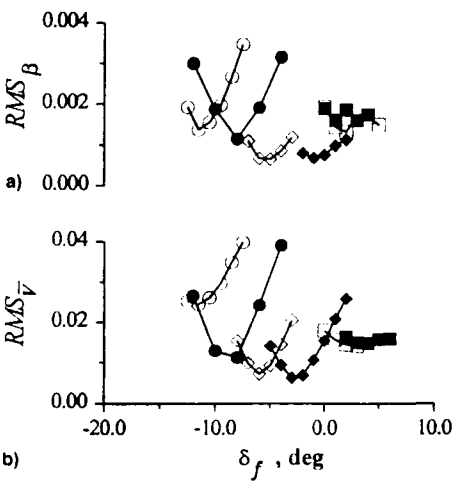

Fig. 11 Variation in the RMS values for different angles of attack and flap settings for hybrid airfoil B (see Fig. 10 for key symbols).

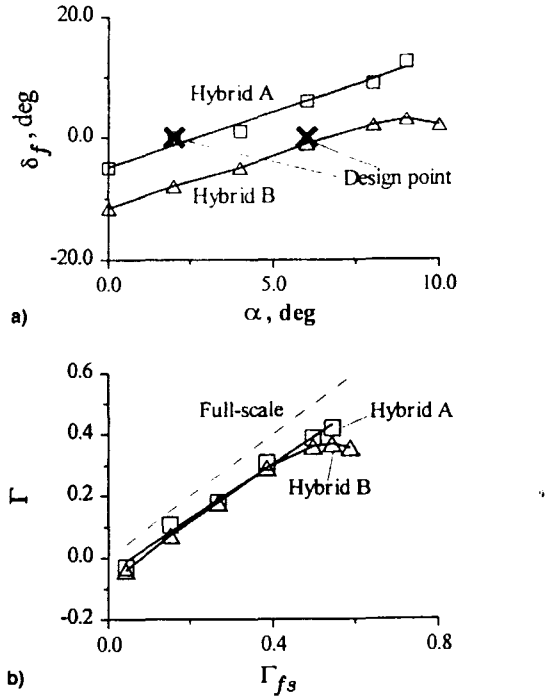

Fig. 12 Plot of a) optimum flap deflection and b) respective airfoil circulation.

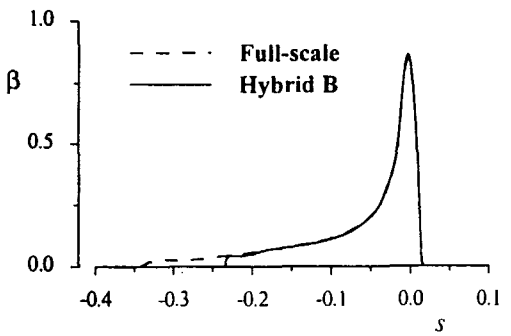

Fig. 13 Comparison of off-design β for 40-μm droplet size at α = 4 deg and δ_f = −5 deg.

airfoils with that of the full-scale airfoil. The results indicate that the hybrid airfoils require less circulation than the full-scale airfoil to simulate full-scale droplet impingement, and that the difference between the full-scale and hybrid airfoil circulation is nearly constant until significant flow separation occurs on the hybrid airfoils. Beyond this point the hybrid airfoil circulation starts to fall off gradually and, therefore, suggests the limit to which a hybrid airfoil can be used to simulate full-scale droplet-impingement characteristics.

It is important to note in Figs. 10 and 11 that the $RMS_{\bar{v}}$ values are an order of magnitude higher than the corresponding RMS_{β}. Although contributions to the RMS values caused by numerical noise cannot be ruled out completely, differences in surface velocity may affect the thermodynamics of ice accretion. Thus, it becomes necessary to incorporate the ice accretion process in the design method, in addition to flow and droplet-impingement analysis.

The effect of larger droplet size on the off-design simulation is shown in Fig. 13. Similar trends can be observed as in the on-design case. Because large-sized droplets result in an increase in the limits of impingement, they, together with the angle of attack of interest, may dictate the size of the nose section and, thus, limit the range of application of the present method.

Conclusions

From this work it has been shown that it is possible to design hybrid airfoils with full-scale leading edges and redesigned aft sections that exhibit full-scale airfoil water droplet-impingement characteristics throughout a given angle-of-attack range. The results indicate the usefulness of a flap system in simulating off-design full-scale droplet-impingement characteristics. The use of a flap for full-scale droplet-impingement simulation is, however, restricted to low and moderate angles of attack, because at high absolute angles of attack together with high flap deflections, the hybrid airfoils become susceptible to flow separation. It should be possible to overcome this limitation, however, by the use of a more sophisticated flap system or by the application of boundary-layer control methods.

The results of the off-design simulation also reveal the existence of small differences in surface velocity distribution within the limits of droplet impingement. Because this difference in surface velocity will affect the thermodynamics of ice accretion and prevent full-scale ice-accretion simulation, the present method should be modified to include also the effects of ice accretion in the design of hybrid airfoils.

Acknowledgments

This work was sponsored by NASA Lewis Research Center under Grant NCC3-408. We would like to thank Reuben Chanderasekharan of Learjet, Inc., for providing the NASA Lewis Research Center with the Learjet GLC 305 airfoil used in this study. Also, helpful discussions with Gene Addy, Tom Ratvasky, and Tom Bond of NASA Lewis Research Center are gratefully acknowledged.

References

[1]Anon., "Selected Bibliography of NACA–NASA Aircraft Icing Publications," NASA TM 81651, Aug. 1981.

[2]Anon., "Icing Technology Bibliography," Society of Automotive Engineers, Aerospace Information Rept. 4015, Warrendale, PA, Nov. 1987.

[3]Anon., "Aircraft Icing," NASA CP 2086, FAA-RD-78-109, NASA Lewis Research Center, Cleveland, OH, July 1978.

[4]Brun, R. J., "Icing Problems and Recommended Solutions," AGARDograph 16, Nov. 1957.

[5]Perkins, P., and Rieke, W., "Aircraft Icing Problems—After 50 Years," AIAA Paper 93-0392, Jan. 1993.

[6]Bragg, M. B., Gregorek, G. M., and Shaw, R. J., "An Analytical Approach to Airfoil Icing," AIAA Paper 81-0403, Jan. 1981.

[7]Bragg, M. B., "Effect of Geometry on Airfoil Icing Characteristics," *Journal of Aircraft*, Vol. 21, No. 7, 1984, pp. 505–511.

[8]Ruff, G. A., "Verification and Application of the Icing Scaling Equations," AIAA Paper 86-0481, Jan. 1986.

[9]Bilanin, A. J., "Proposed Modifications to Ice Accretion/Icing Scaling Theory," AIAA Paper 88-0203, Jan. 1988.

[10]Anderson, D. N., "Rime-, Mixed- and Glaze-Ice Evaluations of Three Scaling Laws," AIAA Paper 94-0718, Jan. 1994.

[11]Anderson, D. N., "Methods for Scaling Icing Test Conditions," AIAA Paper 95-0540, Jan. 1995.

[12]Von Glahn, U. H., "Use of Truncated Flapped Airfoils for Impingement and Icing Tests of Full-Scale Leading-Edge Sections," NACA RM E56E11, July 1956.

[13]Saeed, F., Selig, M. S., and Bragg, M. B., "Design of Subscale Airfoils with Full-Scale Leading Edges for Ice Accretion Testing," *Journal of Aircraft*, Vol. 34, No. 1, 1997, pp. 94–100.

[14]Theodoreson, T., and Garrick, I. E., "General Potential Theory of Arbitrary Wing Sections," NACA Rept. 452, Jan. 1934.

[15]Woan, C. J., "Fortran Programs for Calculating the Incompressible Potential Flow About a Single Element Airfoil Using Conformal Mapping," Aeronautical and Astronautical Research Lab., Ohio State Univ., TR AARL 80-02, Columbus, OH, Jan. 1980.

[16]Selig, M. S., and Maughmer, M. D., "A Multipoint Inverse Airfoil Design Method Based on Conformal Mapping," *AIAA Journal*, Vol. 30, No. 5, 1992, pp. 1162–1170.

[17]Eppler, R., "Direct Calculation of Airfoils from Pressure Distribution," NASA Technical Translation F-15, 417, March 1974, translated from *Ingenieur–Archive*, Vol. 25, No. 1, 1957, pp. 32–57.

[18]Eppler, R., and Somers, D. M., "A Computer Program for the Design and Analysis of Low-Speed Airfoils," NASA TM-80210, Aug. 1980.

[19]Eppler, R., *Airfoil Design and Data*, Springer-Verlag, New York, 990.

[20]Drela, M., and Giles, M. B., "ISES: A Two-Dimensional Viscous Aerodynamic Design and Analysis Code," AIAA Paper 87-0424, Jan. 1987.

[21]Drela, M., "Low-Reynolds Number Airfoil Design for the MIT Daedalus Prototype: A Case Study," *Journal of Aircraft*, Vol. 25, No. 8, 1988, pp. 724-732.

[22]Drela, M., "XFOIL: An Analysis and Design System for Low Reynolds Number Airfoils," *Lecture Notes in Engineering: Low Reynolds Number Aerodynamics*, edited by T. J. Mueller, Vol. 54, Springer-Verlag, New York, 1989, pp. 1-12.

[23]Taylor, G. I., "Notes on Possible Equipment and Technique for Experiments on Icing on Aircraft," Aeronautical Research Council, R&M 2024, Jan. 1940.

[24]Glauert, M., "A Method of Constructing the Paths of Raindrops of Different Diameters Moving in the Neighbourhood of (1) a Circular Cylinder, (2) an Aerofoil Placed in a Uniform Stream of Air; and a Determination of the Rate of Deposit of the Drops on the Surface and the Percentage of Drops Caught," Aeronautical Research Council, R&M 2025, Nov. 1940.

[25]Langmuir, I., and Blodgett, K. B., "A Mathematical Investigation of Water Droplet Trajectories," U.S. Army Air Forces, TR 5418, Feb. 1946.

[26]Bragg, M. B., "A Similarity Analysis of the Droplet Trajectory Equation," *AIAA Journal*, Vol. 20, No. 12, 1982, pp. 1681-1686.

[27]Bragg, M. B., "AIRDROP: Airfoil Droplet Impingement Code," NASA CR (to be published).

[28]Bragg, M. B., and Gregorek, G. M., "An Incompressible Droplet Impingement Analysis of Thirty Low and Medium Speed Airfoils," Aeronautical and Astronautical Research Lab., Ohio State Univ., TR AARL 82-02, Columbus, OH, Feb. 1982.

[29]Gent, R. W., "Calculation of Water Droplet Trajectories About an Aerofoil in Steady, Two-Dimensional, Compressible Flow," Royal Aircraft Establishment, TR 84060, Farnborough, Hants, UK, June 1984.

[30]Saeed, F., and Selig, M. S., "A Multipoint Inverse Design of Airfoils with Slot-Suction," *Journal of Aircraft*, Vol. 33, No. 5, 1996, pp. 708-715.

[31]Saeed, F., and Selig, M. S., "A New Class of Airfoils Using Slot-Suction," AIAA Paper 96-0058, Jan. 1996.